# 2-D HISTOGRAM BASED ON RELATIVE ENTROPY THRESHOLDING FOR CROP SEGMENTATION USING UAV-BASED IMAGES

**Gattu Priyanka**[1], **P Rajalakshmi**[1], **Jana Kholova**[2]

[1]Department of Electrical Engineering, Indian Institute of Technology Hyderabad, Hyderabad, 502285, Telangana, India.
[2]Crops Physiology & Modeling, Accelerated Crop Improvement Research Theme, International Crops Research Institute for the Semi-Arid Tropics (ICRISAT), Hyderabad, 502324, Telangana, India.

**Abstract**

Recently, Unmanned aerial vehicle (UAV) based remote sensing has become a promising way in precision agriculture. Crop or plant segmentation from UAV images plays a vital role in monitoring crop growth. However, the extraction of crops under various illumination conditions is onerous. Numerous methods on segmentation were presented in the literature, out of which threshold-based methods are simple and easy to implement. Previous methods used for crop segmentation utilized complete information of pixels in an image resulting in improper segmentation. The use of local information about pixels can give accurate segmentation. In this work, we constructed a two-dimensional histogram utilizing the gray level of pixels and relative entropy of its neighboring pixels. The optimal threshold was obtained by minimizing relative entropy criteria. The crops were extracted using logical AND operator on segmented image and $a^*$ channel of CIELAB color space. The proposed method was evaluated on Sorghum and Pearl Millet datasets. The misclassification error, Dice coefficient, Jaccard Index were used to compare the performance of the proposed method, Otsu, and Kapur method. The performance analysis shows that the proposed approach achieved more accurate segmentation than other threshold-based methods.

## Introduction

Advanced accelerated crop improvement techniques are required to appease the global food demand (Elferink and Schierhorn 2016; Agrimonti, Lauro, and Visioli 2021). Recent advancements in technology require crop phenotyping and monitoring for the research and development of crops. Digital imaging has evolved as a foundation to capture plant information for the development of automated or semi-automated approaches (Zhao et al. 2019). In recent years, UAV-based imaging has become beneficial in monitoring and assessing features of crops (Xie and Yang 2020). The usage of UAV-based imagery is rapidly becoming more prevalent in precision agriculture.

Besides data acquisition through sensors, crop segmentation plays a pivotal role in monitoring plant growth and health. Segmenting the crop from background is the primary step that aids in addressing crop traits such as plant count (Mukhtar et al. 2021; García-Martínez et al. 2020), LAI (Roth et al. 2018), weed identification (Fawakherji et al. 2019; Bakhshipour et al. 2017), which help in crop improvement programs. The estimation of crop traits depends on the accuracy of segmentation. The segmentation process separates different pixels in the acquired images into crops and background (soil, weeds, irrigation pipes, etc.). However, crop segmentation in fields under varying illumination and weather conditions is onerous and is an open challenge.

There exists considerable research on crop segmentation. Popular methods used for crop segmentation are color-index-based, threshold-based, and learning-based. Color transformations of RGB image to CIELAB, HSV were used to extract the crops (Riehle, Reiser, and Griepentrog 2020; Hassanein, Lari, and El-Sheimy 2018), but this produces over-segmentation of crops in a particular channel. Indices such as Excess Green (ExG), Excess Green minus Excess Red (ExGR), Triangular greenness index (TGI), Vegetative index (VEG), Color Index of Vegetation (CIVE) and fusion indices such as COM1, COM2, combined with thresholding methods like Otsu, Kapur 's, were used to obtain crops from background (Suh, Hofstee, and van Henten 2020; Otsu 1979; Kapur, Sahoo, and Wong 1985). Index-based methods are easy to implement yet not valid for all crops under different illumination conditions. Different learning-based methods such as SVMs, SegNet, ResNet, UNet architectures have been used for crop segmentation (Fawakherji et al. 2019; Cai et al. 2021; Rico-Fernández et al. 2019; Yue et al. 2020). Although the learning methods can segment the crops under different illumination conditions, they are computationally expensive and require frequent training on new datasets. Simple and efficacious segmentation methods are desirable in practice. Among the methods mentioned above, threshold-based methods are effective and easy to implement. The threshold methods used in literature used only the brightness information of pixels in the whole image, thus resulting in poor segmentation. Considering information among pixels aids in accounting brightness information locally, resulting in accurate segmentation.

Authors in (Xiao, Cao, and Zhang 2008) constructed a GLSC histogram utilizing the gray value of the original image and their similarity with its neighbors in a given neighborhood. A two-dimensional orientation histogram was proposed in (Yimit et al. 2013), using gradient orientations of

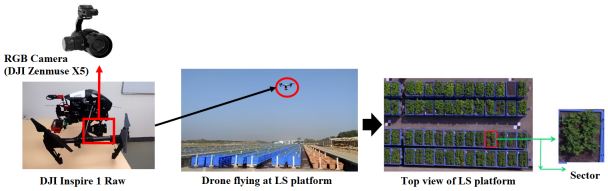


Figure 1: Data Acquisition from UAV-RGB camera setup at LS platform.

each point in a neighborhood. A 2-D histogram was created using the original image and weighted mean filtered image in (Jiang et al. 2018). In (Zheng, Ye, and Tang 2017), a GLLV histogram was developed using the gray level of pixel and its local variance in an image. Authors in (Yang, Cai, and Wu 2020) utilized gray level of the original image and the relative entropy of its neighbors to create a two-dimensional histogram.

Motivated by the idea in (Yang, Cai, and Wu 2020), here, in this study, we construct a two-dimensional histogram utilizing the gray level of original image and modified relative entropy as in (Yang, Cai, and Wu 2020). The optimal threshold for segmentation was achieved by minimizing the relative-entropy criterion. The rest of the paper is structured as follows: Data Acquisition and pre-processing are outlined in Section 2. Section 3 summarizes the proposed method, and Section 4 includes experimental results. Section 5 summarizes this work and addresses directions for future research.

## Data Acquisition and Pre-Processing

For this, the images were acquired with DJI Zenmuse X5 RGB camera mounted on a UAV (DJI Inspire 1 Raw) over the LeasyScan (LS) platform at International Crops Research Institute for Semi-Arid Tropics (ICRISAT), Hyderabad, India, as shown in Figure 1. The UAV was programmed at a speed of $5km/hr$ periodically at the height of $10m$, with $80\%$ overlap between two consecutive images in autopilot mode. The images were captured at every two seconds interval during the entire flight of the UAV. The LS platform consists of $4800$ sectors where each sector (Figure 1) is one experimental unit planted with one genotype. A brief description of the LS platform can be found at (Vadez et al. 2015).

The images captured through UAV were processed using Agisoft Photoscan (LLC 2020) tool to create an orthomosaic. Then, a fishnet was created over the orthomosaic through QGIS tool (QGIS Development Team 2022) to extract individual sectors. Each sector is an RGB image consisting of foreground (plants) and background (soil, tray, irrigation pipes). The sectors were well maintained and free from weeds. The region of interest is the crop in each sector, which have to be segmented for further monitoring. The proposed method to segment crops is described in the next section.

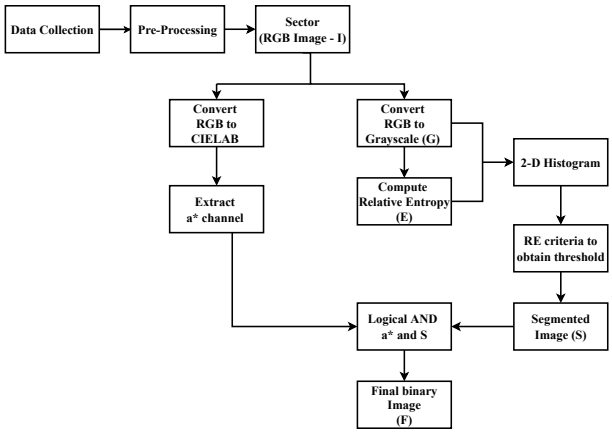


Figure 2: Flow chart of the proposed approach.

## Proposed Method

A two-dimensional histogram was constructed using the gray level of image and relative entropy (RE) of neighboring pixels. The optimal threshold for segmentation was obtained using minimum relative entropy criteria. The crops were extracted using the logical AND operator on segmented image and $a^*$ channel of CIELAB color space. Figure 2 shows the work flow of proposed method.

### Two dimensional histogram

Assume each sector as an RGB image $I(m,n) \in R^{M\times N\times 3}$ and $G(m,n) \in R^{M\times N}$ as corresponding $8-$ bit grayscale image (where, $M$ = width, $N$ = height) respectively. Each pixel in $G(m,n)$ corresponds to gray level in that image. RE of $G(m,n)$ in $k\times k$ neighborhood is defined in Equation (1). The RE for each pixel was normalized between $0$ to $L-1$ as in Equation (2).

$$E(m,n) = \sum_{i=-(k-1)/2}^{(k+1)/2} \sum_{j=-(k-1)/2}^{(k+1)/2} A\times \mid \log \frac{A}{B} \mid \qquad (1)$$

$$E(m,n) = \left( \frac{E(m,n) - E_{min}}{E_{max} - E_{min}} \right) \times (L-1) \qquad (2)$$

where, $E(m,n)$ represents RE of grayscale image $G(m,n)$, $A = G(m+i, n+j)$, $B$ = median of $G(m+i, n+j)$ in neighbourhood $k \times k$, $E_{min}$ and $E_{max}$ are the minimum and maximum value of $E(m,n)$ respectively. The use of median gives the intensity value present in the local image, and preserves the edges in an image.

Next, a two dimensional histogram was constructed by computing the number of pixel pairs between original grayscale image and RE of grayscale image, i.e., $G(m,n) = i$ and $E(m,n) = j$, which is denoted as $h_{ij}$. Then, the histogram which is of size $L \times L$ is computed using Equation (3).

$$P_{ij} = \frac{h_{ij}}{M \times N} \qquad (3)$$

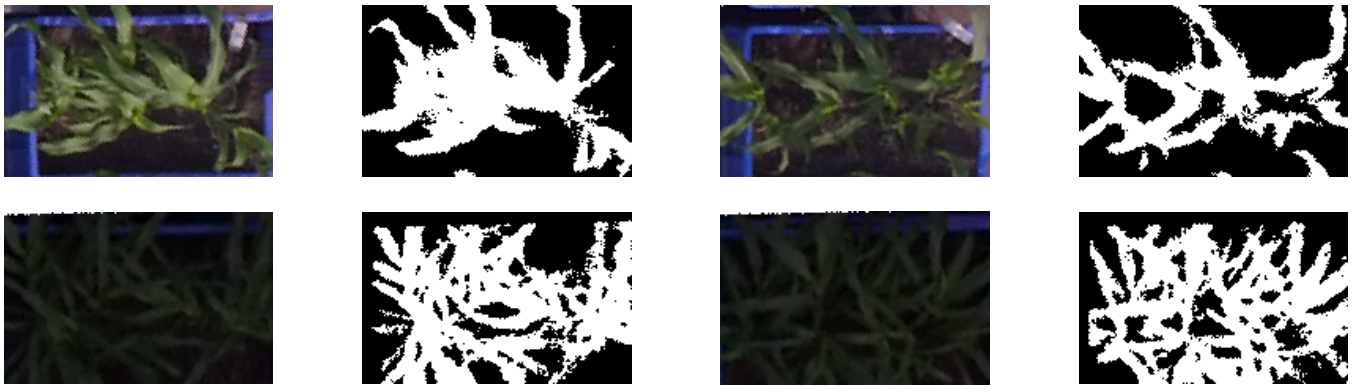

Figure 3: The test images and their groundtruth: Top - Sorghum 1, Sorghum2, Bottom - Pearl Millet 1, Pearl Millet 2.

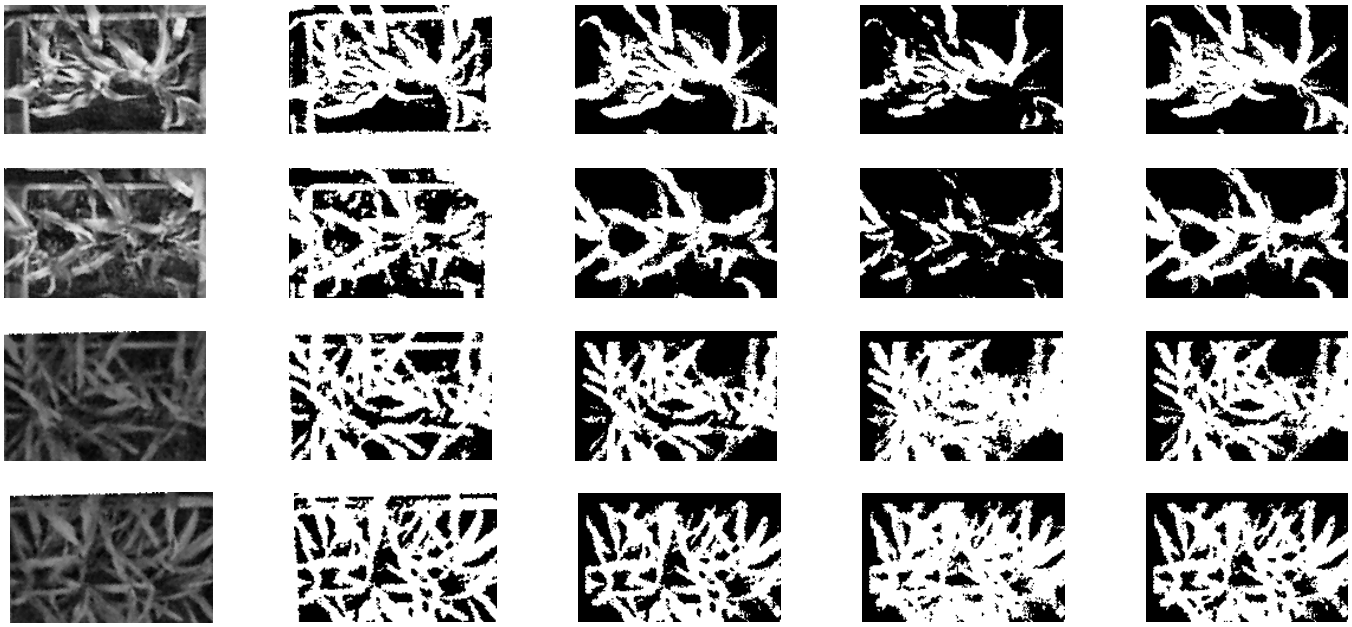

(a) (b) (c) (d) (e)

Figure 4: Segmentation results of sample test images: (a) Grayscale, (b) Proposed method - segmented image(S), (c) Proposed method- final binary image (F), (d) Otsu, (e) Kapur.

Table 1: Segmentation performance of the proposed method with different metrics

| **Sample Images** | **ME** | | | **Dice Coefficient** | | | **Jaccard Index** | | |
|---|---|---|---|---|---|---|---|---|---|
| | **Otsu** | **Kapur** | **Proposed method** | **Otsu** | **Kapur** | **Proposed method** | **Otsu** | **Kapur** | **Proposed method** |
| Sorghum 1 | 0.1740 | 0.4200 | **0.0679** | 0.7389 | 0.6822 | **0.9050** | 0.5860 | 0.5912 | **0.8264** |
| Sorghum 2 | 0.1735 | 0.3676 | **0.0576** | 0.6570 | 0.7214 | **0.9099** | 0.5693 | 0.6446 | **0.8341** |
| Pearl Millet 1 | 0.1529 | 0.0171 | **0.0012** | 0.8001 | 0.8819 | **0.9353** | 0.6598 | 0.7653 | **0.8785** |
| Pearl Millet 2 | 0.5523 | 0.4137 | **0.2523** | 0.5925 | 0.6993 | **0.8022** | 0.4209 | 0.5009 | **0.7122** |

### Relative Entropy Criteria for segmentation

The threshold was obtained by minimizing the relative entropy. This threshold was used to segment the objects and soil. Let $g, e$ be the threshold for image $G$ and RE image $E$, respectively. The two-dimensional relative entropy between $G$ and its segmented version at $(g, e)$ is calculated as;

$$D(P,Q|,g,e) = \sum_{i=0}^{g-1}\sum_{j=0}^{e-1}\left(iP_{ij}\log\frac{i}{\mu_{0i}} + jP_{ij}\log\frac{j}{\mu_{0j}}\right) + \sum_{i=g}^{L-1}\sum_{j=0}^{e-1}\left(iP_{ij}\log\frac{i}{\mu_{1i}} + jP_{ij}\log\frac{j}{\mu_{1j}}\right) \quad (4)$$

where, $\mu_0, \mu_1$ are the mean vector of object and soil class respectively.

Due to space constraints,the detailed formulation of equations were not mentioned. The equations can be referred at (Li and Lee 1993). The optimum threshold value $(g^*, e^*)$ is obtained by minimizing $D(P,Q|,g,e)$ as in Equation (5).

$$(g^*, e^*) = arg\,min\, D(P,Q|,g,e) \quad (5)$$

### Crop Segmentation

The segmented image $(S(m,n))$ of sector was obtained by utilizing the optimal threshold from Equation (5). This segmented image consists of the crops along with sector border as shown in Figure 4(b). Since only plants are the region of interest, a mask was created by extracting $a^*$ channel from CIELAB color space. A binary image (F) representing plants as white pixels and background as black pixels was obtained by applying the logical AND operator on $a^*$ channel and segmented image (S) as shown in Figure 4(c).

## Results and Discussion

The performance of the proposed approach was measured using misclassification error ($ME$, Equation (6)) (Chaira 2012), $Dice\ coefficient$ (Equation (7)), and $Jaccard\ Index$ (Equation (8)) on the sorghum and pearl millet dataset obtained through UAV-camera setup.

$$ME = 1 - \frac{|Back_g \cap Back_{th}| + |Fore_g \cap Fore_{th}|}{|Back_g| + |Fore_g|} \quad (6)$$

$$Dice\,Coefficient = 2 * \frac{|A_1 \cap A_2|}{|A_1| + |A_2|} \quad (7)$$

$$Jaccard\,Index = \frac{|A_1 \cap A_2|}{|A_1 \cup A_2|} \quad (8)$$

where, $|.|$ indicate the number of elements in the set, $Back_g$, $Back_{th}$ represents number of background pixels of ground truth and Final thresholded image, $Fore_g$, $Fore_{th}$ represents number of foreground pixels of ground truth and Final thresholded image in Equation (6) respectively. $A_1$, $A_2$ represent the ground truth and final thresholded image in Equation (7), (8) respectively.

The values of $ME$, $Dice\ Coefficient$, and $Jaccard\ Index$ are in the range $[0, 1]$. $ME$ close to 0 and $Dice\ Coefficient$, $Jaccard\ Index$ close to 1 indicates better segmentation results. The segmentation results were compared with ground truth to evaluate the performance. The analysis was carried out in MATLAB 2019a. We tested on fifty sectors from each dataset. The sorghum dataset has images considerably brighter than the pearl millet dataset. Due to space constraints, we presented the results of only sample sectors of sorghum and pearl millet crop with their corresponding ground truth as shown in Figure 3. The ground truth was generated using Adobe Photoshop. All the sectors were of size $171 \times 109$. The modified relative entropy used in this work utilizes the median of a local image instead of the mean as in (Yang, Cai, and Wu 2020). The median gives the intensity value present in the local image, whereas the mean may give other intensity values which may result in poor segmentation results. We also tested by considering various neighborhoods ($3 \times 3$, $5 \times 5$, $7 \times 7$) and obtained optimal results at $3 \times 3$ neighborhood. One can observe that darker images resulted in poor segmentation than bright images (Figure 4, Table 1). The performance of the proposed method was compared with Otsu (Otsu 1979), Kapur (Kapur, Sahoo, and Wong 1985) criteria, and the results were presented in Table 1. The proposed method shows better segmentation results as compared to Otsu and Kapur methods. The Otsu method performed under segmentation, whereas the Kapur method performed over-segmentation.

Finally, the proposed approach accurately segments crops from the background and can be used for further analysis (such as estimation of canopy coverage, and leaf area index) in crop improvement programs.

## Conclusion

We presented a novel method for crop segmentation from UAV images using a relative entropy histogram. The proposed method considers local information of images and accurately segments the crops in a brighter as well as darker luminance environment. This method was easy to implement and tested on sorghum and pearl millet crops and can further extend to other crops like chickpea, mungbean, groundnut.

## References


Agrimonti, C.; Lauro, M.; and Visioli, G. 2021. Smart agriculture for food quality: facing climate change in the 21st century. *Critical reviews in food science and nutrition*, 61(6): 971–981.

Bakhshipour, A.; Jafari, A.; Nassiri, S. M.; and Zare, D. 2017. Weed segmentation using texture features extracted from wavelet sub-images. *Biosystems Engineering*, 157: 1–12.

Cai, W.; Wei, Z.; Song, Y.; Li, M.; and Yang, X. 2021. Residual-capsule networks with threshold convolution for segmentation of wheat plantation rows in UAV images. *Multimedia Tools and Applications*, 80(21): 32131–32147.

Chaira, T. 2012. Intuitionistic fuzzy color clustering of human cell images on different color models. *Journal of Intelligent & Fuzzy Systems*, 23(2-3): 43–51.

Elferink, M.; and Schierhorn, F. 2016. Global demand for food is rising. Can we meet it. *Harvard Business Review*, 7(04): 2016.

Fawakherji, M.; Youssef, A.; Bloisi, D.; Pretto, A.; and Nardi, D. 2019. Crop and weeds classification for precision agriculture using context-independent pixel-wise segmentation. In *2019 Third IEEE International Conference on Robotic Computing (IRC)*, 146–152. IEEE.

García-Martínez, H.; Flores-Magdaleno, H.; Khalil-Gardezi, A.; Ascencio-Hernández, R.; Tijerina-Chávez, L.; Vázquez-Peña, M. A.; and Mancilla-Villa, O. R. 2020. Digital count of corn plants using images taken by unmanned aerial vehicles and cross correlation of templates. *Agronomy*, 10(4): 469.

Hassanein, M.; Lari, Z.; and El-Sheimy, N. 2018. A new vegetation segmentation approach for cropped fields based on threshold detection from hue histograms. *Sensors*, 18(4): 1253.

Jiang, C.; Yang, W.; Guo, Y.; Wu, F.; and Tang, Y. 2018. Nonlocal means two dimensional histogram-based image segmentation via minimizing relative entropy. *Entropy*, 20(11): 827.

Kapur, J. N.; Sahoo, P. K.; and Wong, A. K. 1985. A new method for gray-level picture thresholding using the entropy of the histogram. *Computer vision, graphics, and image processing*, 29(3): 273–285.

Li, C. H.; and Lee, C. 1993. Minimum cross entropy thresholding. *Pattern recognition*, 26(4): 617–625.

LLC, A. 2020. Agisoft Metashape user manual— Professional edition, version 1.6. https://www.agisoft.com/pdf/metashape-pro_1_6_en.pdf. Accessed: 2022-11-10.

Mukhtar, H.; Khan, M. Z.; Khan, M. U. G.; Saba, T.; and Latif, R. 2021. Wheat Plant Counting Using UAV Images Based on Semi-supervised Semantic Segmentation. In *2021 1st International Conference on Artificial Intelligence and Data Analytics (CAIDA)*, 257–261. IEEE.

Otsu, N. 1979. A threshold selection method from gray-level histograms. *IEEE transactions on systems, man, and cybernetics*, 9(1): 62–66.

QGIS Development Team. 2022. *QGIS Geographic Information System*. QGIS Association.

Rico-Fernández, M.; Rios-Cabrera, R.; Castelán, M.; Guerrero-Reyes, H.-I.; and Juarez-Maldonado, A. 2019. A contextualized approach for segmentation of foliage in different crop species. *Computers and Electronics in Agriculture*, 156: 378–386.

Riehle, D.; Reiser, D.; and Griepentrog, H. W. 2020. Robust index-based semantic plant/background segmentation for RGB-images. *Computers and Electronics in Agriculture*, 169: 105201.

Roth, L.; Aasen, H.; Walter, A.; and Liebisch, F. 2018. Extracting leaf area index using viewing geometry effects—A new perspective on high-resolution unmanned aerial system photography. *ISPRS Journal of Photogrammetry and Remote Sensing*, 141: 161–175.

Suh, H. K.; Hofstee, J. W.; and van Henten, E. J. 2020. Investigation on combinations of colour indices and threshold techniques in vegetation segmentation for volunteer potato control in sugar beet. *Computers and Electronics in Agriculture*, 179: 105819.

Vadez, V.; Kholová, J.; Hummel, G.; Zhokhavets, U.; Gupta, S.; and Hash, C. T. 2015. LeasyScan: a novel concept combining 3D imaging and lysimetry for high-throughput phenotyping of traits controlling plant water budget. *Journal of Experimental Botany*, 66(18): 5581–5593.

Xiao, Y.; Cao, Z.; and Zhang, T. 2008. Entropic thresholding based on gray-level spatial correlation histogram. In *2008 19th International Conference on Pattern Recognition*, 1–4. IEEE.

Xie, C.; and Yang, C. 2020. A review on plant high-throughput phenotyping traits using UAV-based sensors. *Computers and Electronics in Agriculture*, 178: 105731.

Yang, W.; Cai, L.; and Wu, F. 2020. Image segmentation based on gray level and local relative entropy two dimensional histogram. *Plos one*, 15(3): e0229651.

Yimit, A.; Hagihara, Y.; Miyoshi, T.; and Hagihara, Y. 2013. 2-D direction histogram based entropic thresholding. *Neurocomputing*, 120: 287–297.

Yue, Y.; Li, X.; Zhao, H.; and Wang, H. 2020. Image Segmentation Method of Crop Diseases Based on Improved Segnet Neural Network. In *2020 IEEE International Conference on Mechatronics and Automation (ICMA)*, 1986–1991. IEEE.

Zhao, C.; Zhang, Y.; Du, J.; Guo, X.; Wen, W.; Gu, S.; Wang, J.; and Fan, J. 2019. Crop phenomics: current status and perspectives. *Frontiers in Plant Science*, 10: 714.

Zheng, X.; Ye, H.; and Tang, Y. 2017. Image bi-level thresholding based on gray level-local variance histogram. *Entropy*, 19(5): 191.